Kinetics analysis and simulation of sequential epoxy dual-curing systems with independent thermal activation

David Santín, Osman Konuray, Xavier Fernàndez-Francos,* Xavier Ramis

Thermodynamics Laboratory, ETSEIB, Universitat Politècnica de Catalunya, Av. Diagonal 647, 08028, Barcelona, Spain.

*Corresponding author: xavier.fernandez@upc.edu
Phone: +34 934017955
Fax: +34 934017389

ABSTRACT

The curing kinetics of a sequential dual-curing system based on an off-stoichiometric amine-epoxy formulation with intermediate latent reactivity has been analyzed. The first curing stage is an epoxy-amine polycondensation taking place at low temperatures, while the second curing stage is an anionic homopolymerization of the excess epoxy groups, taking place at high temperatures and catalyzed by a latent base. The different reactivity of both polymerization processes allows an excellent separation into well-defined curing stages each of which can be analyzed individually. The kinetics of the two curing stages have been analyzed by integral isoconversional procedures and model-fitting methods. Both methodologies successfully simulated each curing stage and also the global curing process, showing that it is possible to control the activation of both curing stages. Isoconversional integral analysis is a simple yet powerful method that can be used for the simulation of temperature-controlled curing programmes. Model-fitting analysis is more suitable for the flexible simulation of processing scenarios such as the curing of composites.

Keywords: epoxy; amine; dual-curing; latent base; thermosets; kinetics analysis

1 INTRODUCTION

Sequential dual-curing, combining two different polymerization processes taking place in a controlled and sequential way in a curing process, is a highly advantageous technology for the processing of thermosetting systems [1]. This technology is highly versatile and flexible due 1) to the possibility of controlling the curing sequence using different stimuli (i.e. UV-light, temperature) and 2) the ability to tailor intermediate and final network structures and properties [2-5]. Click-type or non-click reactions can be used and combined in sequential dual-curing systems [1]. Due to their high versatility, acrylate [3, 6-10], ene [5, 11] and epoxy [2, 4, 5, 12, 13] reactions are commonly used in dual-curing systems.

A novel off-stoichiometric epoxy-amine system, with excess epoxy groups and latent reactivity in the intermediate state was recently reported [2]. The first curing reaction was a self-limiting epoxy-amine condensation that takes place at moderate temperatures until exhaustion of reactive amine groups. In this system, Jeffamine (a diamine with a polyether backbone) was used as amine curing agent for the curing of diglycidyl ether of bisphenol A (DGEBA) in the first curing stage. A controlled excess of DGEBA allowed the preparation of a family of materials with a wide range of intermediate and final properties [2]. The use of 1-methylimidazolium tetraphenylborate (1MI-Ph_4B) as latent thermal base for the epoxy homopolymerization ensured at least 7 weeks of storage stability at 30 ºC for intermediate materials after the completion of the epoxy-amine reaction [2]. A time-temperature-transformation (TTT) diagram summarizing the isothermal curing kinetics of this dual-curing system with 50 % excess of DGEBA was recently reported [14]. The different reactivity of the curing stages and the possibility of controlling each curing reaction at different temperatures were demonstrated with the help of it. The intermediate materials had remarkable storage stability prior to the activation of the second curing stage. The apparent overlapping between the curing processes under constant heating rate conditions [14], caused by the somewhat low reactivity of Jeffamine, precluded the analysis of the curing kinetics from a global point of view. Therefore the curing kinetics of each curing stages was analyzed separately, under safe temperature conditions. Only isoconversional kinetics analysis based on isothermal kinetic data was performed. The TTT and the conversion-temperature-transformation (CTT) diagrams also evidenced the differences between both curing processes in terms of network build-up [14].

In the present work we have analyzed a dual-curing epoxy system based on diethylenetriamine (DETA) as amine curing agent and DGEBA, with an amine-epoxy ratio of 0.4 and 4 phr (parts per hundred) of 1MI-Ph_4B as latent initiator for the homopolymerization of excess epoxy groups in the second curing stage. The combination of a latent initiator and a high reactivity aliphatic amine such as DETA should allow a better separation between curing stages than in previously reported systems [12, 14]. Differential scanning calorimetry (DSC) has been used to obtain kinetic information under isothermal and nonisothermal conditions. The nonisothermal curing kinetics of the global curing process have been analyzed using isoconversional integral methods. Isothermal and nonisothermal data has been combined in the individual analyses of the curing stages by the isoconversional integral method and model fitting methodology. The simulation of global curing process using isoconversional and model-fitting methods is also performed and compared with experimental data.

2 EXPERIMENTAL

2.1 Materials

Diglycidyl ether of bisphenol A (DGEBA, M_w=374 g/mol or M_w=187 g/ee, Epikote^{TM}) was kindly supplied by Hexion speciality Chemical B.V. and dried in vacuum before use. Diethylenetriamine (DETA, M_w=103.2 g/mol or M_w=20.6 g/eq), 1-methylimidazole (1MI) and sodium tetraphenylborate ($NaBPh_4$) were supplied by Aldrich and used as received. Methanol (MeOH) and chloroform ($CHCl_3$) were supplied by VWR and were used as received. 1M1·$HBPh_4$ (BG hereafter) was prepared using the procedure outlined in the literature [14-16]. The structures of DG, DETA and BG are shown in Scheme 1.

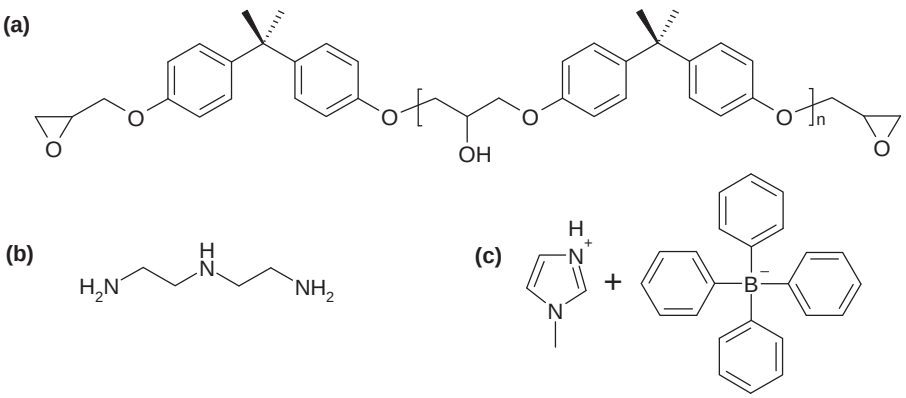

Scheme 1: Molecular structures of the chemicals used: (a) DGEBA, (b) DETA and (c) 1MI·$HBPh_4$ (BG).

2.2 Preparation of the curing mixtures

Samples were prepared in 5 mL vials in 1-2 gr batches using the following procedure: BG was weighed and added to DG and was kept under agitation at 90 ºC for 15 min at complete solubilization. The mixture was left to cool down to room temperature after which the required amount of DETA was added, quickly stirred and immediately sent to analysis or sample preparation. A formulation was prepared with an amine-epoxy ratio of 0.4, that is, with a 60 % excess of epoxy groups. 4 phr of BG were used. The composition of the formulation is shown in Table 1.

Table 1: Composition of the formulation studied in this work.

$DGEBA\ (wt.\%)$	92.10
$DETA\ (wt.\%)$	4.06
$BG\ (wt.\%)$	3.84
eq_{DETA}/ee	0.4
eq_{BG}/ee	0.0194

2.3 Experimental techniques

Differential scanning calorimeters (DSC) Mettler DSC822e equipped with a robotic arm and with liquid nitrogen cooling, and Mettler DSC821e, were used. The equipments were calibrated using indium (temperature, heat flow) and zinc (temperature) standards. Approximately 10 mg samples were cured in aluminium pans with pierced lids under a nitrogen atmosphere. The DSC822e was used to study the nonisothermal curing at 10 ºC/min up to 300 ºC and the DSC821e was used to study the isothermal curing at temperatures in the range of 70-100 ºC for the first curing process, and 150-210 ºC for the second curing process after precuring of the samples at 90 ºC for 40 minutes in order to complete the first curing process. The calorimetric degree of cure, x, and the reaction rate, dx/dt, were calculated as follows:

$$x = \frac{\Delta h_T}{\Delta h_{total}} \quad or \quad x = \frac{\Delta h_t}{\Delta h_{total}} \qquad (1)$$

$$\frac{dx}{dt} = \frac{dh/dt}{\Delta h_{total}} \qquad (2)$$

where Δh_T and Δh_t are the heat evolved up to a a temperature T or time t during a dynamic or isothermal curing experiment, respectively. Δh_{total} is the total heat released during curing and dh/dt is the instantaneous heat flow released.

The glass transition temperature of the uncured formulation T_{g0} was determined using the DSC822e in the dynamic curing at 10ºC/min starting at -100ºC. The intermediate glass transition temperature (T_{gint}) of the dual system was determined in a dynamic scan at 10 ºC/min after isothermal curing at 90 ºC for 40 minutes. The ultimate glass transition temperature ($T_{g\infty}$) of the fully cured sample (at 180 ºC for enough time so as to complete the curing process) was determined after two consecutive dynamic scans at 10 ºC/min, the first one to determine the presence of residual heat. The T_g was determined as the midpoint in the heat capacity step during the glass transition. The increase in heat capacity during the glass transition, ΔC_p, was also determined. The DIN method, included in the STARe software by Mettler, was used for these determinations.

3 THEORETICAL

3.1 Curing kinetics analysis

Isoconversional analysis (global)

The isoconversional methodology was used for the determination of the apparent activation energy during the curing process [17]. The basis for this methodology is the assumption that the reaction rate can be expressed as separate functions of conversion *x* and temperature *T* as:

$$\frac{dx}{dt} = k(T) \cdot f(x) \qquad (3)$$

Where $k(T) = k_0 \cdot exp\left(-E/RT\right)$ is the kinetic constant, A is the preexponential factor, E is the activation energy, R is the gas constant and $f(x)$ is the model representing the reaction mechanism governing the curing process. In other words, it is assumed that the reaction mechanism is not affected by the temperature schedule of the curing process.

Therefore, the apparent activation energy at a given degree of conversion E_x can be calculated as follows:

$$\frac{dln(dx/dt)}{dT^{-1}} = \frac{dln(f(x))}{dT^{-1}} + \frac{dln(k(T))}{dT^{-1}} \equiv -\frac{E_x}{R} \qquad (4)$$

This is the basis for the differential or Friedman method. Linear regression of $ln(dx/dt)$ against the inverse of temperature for different experiments at a given degree of conversion, yields the slope $-E_x/R$ and the intercept at the origin $ln(k_{0,x} \cdot f(x))$. Hereinafter, the subscript x indicates that the value is ascribed to a given degre of conversion x.

Rearrangement and integration of the rate expression leads to:

$$g(x) = \int_0^x \frac{dx}{f(x)} = k_0 \cdot \int_0^t exp(-E/R \cdot T) \cdot dt \qquad (5)$$

Under isothermal conditions, this leads to the following expression, taking natural logarithms:

$$\ln t = \ln\left(\frac{g(x)}{k_0}\right) + \frac{E}{R \cdot T} \qquad (6)$$

Representation of $\ln t$ against $(R \cdot T)^{-1}$ for different experiments at a given degree of conversion x yields a straight line with slope E_x and intercept at the origin $\ln\left(g(x)/k_{0,x}\right)$.

In the case of dynamic curing experiments, integration of expression eq. (5) under constant heating rate conditions yields:

$$\frac{g(x)}{k_0} = \frac{1}{\beta} \cdot \int_0^T exp(-E/R \cdot T) \cdot dT = \frac{1}{\beta} \cdot \frac{E}{R} \cdot p(y) \qquad (7)$$

Where β is the heating rate, and $y = E/R \cdot T$ and $p(y)$ is an approximation of the solution of the temperature integral, making use of the more exact approximations such as the ones of Senum and Yang [18], or else the general set of solutions proposed by Starink that can be used for the determination of activation energy from constant heating rate experiments using linear regression methods [19]:

$$p(y) \cong \frac{\exp\left(-A \cdot y + B\right)}{y^k} \qquad (8)$$

The following expression can be derived for this family of linear isoconversional methods:

$$\ln\frac{\beta}{T^k} = \left[\ln\frac{k_0}{g(x)} + (1-k)\cdot\ln\frac{E}{R} + B\right] - \frac{A\cdot E}{R\cdot T} \qquad (9)$$

Representation of $\ln\left(\beta/T^k\right)$ against $-A\cdot(R\cdot T)^{-1}$ for a number of dynamic experiments at given degree of conversion x should produce a straight line with slope E_x and an intercept at the origin from which one can easily derive the factor $\ln\left(g(x)/k_{0,x}\right)$, which can be used in eq. (6) for the simulation of isothermal processes. Note that the full development of eq. (9) was not shown in the literature [19]. The well-known Kissinger-Akahira-Sunose (KAS) method fits this general model with $A = 1$, $B = 0$ and $k = 2$, but a more accurate solution was found with $A = 1.0008$, $B = -0.312$ and $k = 1.92$ [19].

In contrast, one should mention the nonlinear, advanced integral isoconversional methods of Vyazovkin [17]. The advantages of such methods are manifold. To begin with, they can make use of highly accurate solutions of the temperature integral for constant heating rate experiments [20] that cannot be used in conventional linear methods. The temperature integral can be computed numerically making use of the real sample temperature and therefore it is possible to analyse sets of experimental data from arbitrary temperature programmes or taking into account sample temperature deviations from the prescribed programme [21].

The method can be outlined as follows. Assuming the validity of the isoconversional assumptions, the apparent isoconversional activation energy E_x should fulfill the condition $\left(g(x)/k_0\right)_1 = \left(g(x)/k_0\right)_2 = \ldots = \left(g(x)/k_0\right)_{n_{exp}}$ for a set of n_{exp} experiments. This can also be expressed in terms of an objective function (obj) [21] defined as follows:

$$obj = min\left[\sum_i \sum_{j<>i} \frac{\left(g(x)/k_0\right)_i}{\left(g(x)/k_0\right)_j}\right] \qquad (10)$$

For a given a value of E_x, the values of $\left(g(x)/k_0\right)_i$ should be obtained by numerical integration of eq. (5) making use of the real sample temperature. The value of E_x is determined by numerical iteration using a convenient minimization algorithm [21] for the objective function (10). Finally, the factor $g(x)/k_{0,x}$ can be determined as an arithmetic average as:

$$\frac{g(x)}{k_{0,x}} = \frac{1}{n_{exp}} \cdot \sum \left(g(x)/k_0\right)_i \qquad (11)$$

Where n_{exp} is the total number of experiments employed in the analsysis.

An additional advantage of the nonlinear isoconversional integral methods is the possibility of combining isothermal and nonisothermal data in the analysis, which is not common due to the straightforward application of either isothermal or dynamic linear isoconversional methods. This possibility is exploited in this work in order to obtain reliable values of E_x and $g(x)/k_{0,x}$ from a more complete set of experimental data. For the dynamic experiments, the parameters $\left(g(x)/k_0\right)_i$ are calculated for each heating rate using eq. (7) and a suitable expression for $p(y)$ such as the highly precise 4th order Senum and Yang approximation [18]. For the isothermal experiments, $\left(g(x)/k_0\right)_i$ are calculated from eq. (6). Note that, in both cases, temperature deviations from prescribed heating rate or isothermal temperature are neglected. E_x is obtained using the same objective function given by eq. (10), and the same minimization procedure. The factor $g(x)/k_{0,x}$ is also obtained from eq. (11).

Because the integral isoconversional methods produce pairs of values of E_x and $g(x)/k_{0,x}$ for each degree of conversion, it is possible to simulate isothermal curing programmes using eq. (6) or dynamic curing programmes using eq. (7) (by numerical adjustment of T_x for a given degree of conversion x).

The kinetic parameters determined from eqs. (5)-(11) are not equivalent to those determined using the differential method [17, 22] and should not be exchanged unless the

value of the differential apparent isoconversional energy, E_x, remains constant throughout the curing process.

Isoconversional analysis (individual)

A methodology similar to the one described in our previous work for the separate analysis of the two curing processes in a dual-curing system will be used [14]. In the present work, given the similarities with the previously reported dual-curing system [2, 14], we choose to analyze the curing processes independently, and we also assume that the activation of both curing process is independent as well, that is, the second curing process is not activated inmediately after the end of the first one [23, 24] but has its own activation kinetics (i.e. slow thermal decomposition of BG leading to the release of the initiator for the second curing process). This means that the slow activation of BG is already taking place during the first curing process .

The first curing process is analyzed isothermally at conditions at which the second curing process is not yet activated; the second curing process is analyzed using isothermal and dynamic experiments, after precuring of the samples at 90 ºC for 40 min (note that the reaction time is much shorter due to the higher reactivity of DETA in comparison with the Jeffamine used in the previous work [14]).

The indivivdual kinetics analysis of the first curing process would not be affected. Therefore, eq. (6) (isothermal analysis) is used for the determination of the kinetic parameters $\ln\left(g_1(x)/k_{0,1,x}\right)$ and $E_{1,x}$ for a given degree of conversion x_1.

In the case of the second curing process, the thermal history should be taken into consideration in the analysis. In our previous work we showed that the determination of the apparent activation energy $E_{2,x}$ was unaffected by this consideration, providing the thermal history of all the samples was identical [14]. It only modified the value of

$g_2(x)/k_{0,2,x}$ at the beginning of the second curing stage [14]. In the present case the same approach can be followed.

If we call $I_1(x)$ the temperature integral of the precuring stage, we can write, for dynamic experiments:

$$I_2(x) = \frac{g_2(x)}{k_{0,2}} - I_1(x) = \frac{1}{\beta}\cdot\frac{E_2}{R}\cdot p(y_2) \qquad (12)$$

Where $p(y_2)$ is the 4th order Senum and Yang approximation [18], $y_2 = E_2/R\cdot T_2$ and T_2 is the temperature at a given degree of conversion during the second curing process. For isothermal experiments, with constant T_2:

$$I_2(x) = \frac{g_2(x)}{k_{0,2}} - I_1(x) = \exp\left(-\frac{E_2}{R\cdot T_2}\right)\cdot t_2 \qquad (13)$$

Taking into account that all the samples were precured under the same conditions, that is, $I_1(x)$ is identical, the apparent isoconversional energy $E_{2,x}$ must fulfill the condition $I_2(x)_1 = I_2(x)_2 = \ldots = I_2(x)_{n_{exp}}$. An objective function can therefore be defined:

$$obj = \min\left[\sum_i \sum_{j<>i} \frac{I_2(x)_i}{I_2(x)_j}\right] \qquad (14)$$

$E_{2,x}$ is obtained by numerical iteration using a convenient minimization procedure [21] as described above. The parameters $I_2(x)_i$ are calculated for each heating rate and isothermal temperature using eqs. (12) and (13). An average parameter $I_2(x)$ is determined as:

$$I_2(x) = \frac{1}{n_{exp}}\cdot\sum I_2(x)_i \qquad (15)$$

Taking into account that the samples were all precured at the same isothermal temperature T_1 for the same time t_1, one can calculate the factor $g_2(x)/k_{0,2,x}$ as:

$$\frac{g_2(x)}{k_{0,2,x}} = I_2(x) + I_1(x) = I_2(x) + \exp\left(-\frac{E_{2,x}}{R\cdot T_1}\right)\cdot t_1 \qquad (16)$$

It should be noted that, if the samples had been precured at different conditions (isothermal or dynamic), the objective function (14) should have taken into consideration

$g_2(x)/k_{0,2}$ instead of $I_2(x)$. In this case, the calculation of $I_1(x)$ would be necessary for each experiment and iteration step.

Model-fitting analysis

The experimental rate curves were fitted to an empirical, modified multi-term Kamal model inspired in the models employed by other authors [25, 26] shown in eq. (17):

$$\frac{dx}{dt} = f(x,T) = \sum_{i=1}^{k} k_i \cdot x^{m_i} \cdot (1-x)^{n_i} \qquad (17)$$

$$k_i = k_{0,i} \cdot exp\left(-E_i/R \cdot T\right)$$

where m_i and n_i are the exponents of each autocatalytic function, and k_i is an Arrhenius kinetic constant for each autocatalytic process. The number of adjustable parameters is high, as it includes E_i and $k_{0,i}$ for the different k_is and the reaction orders m_i and n_i for each autocatalytic function. We determined the model parameters by multivariate nonlinear regression, with the following error function to be minimized:

$$error = \frac{1}{n}\sum \frac{\left|\left(\frac{dx}{dt}\right)_{exp} - \left(\frac{dx}{dt}\right)_{calc}\right|}{\left(\frac{dx}{dt}\right)_{exp}} \qquad (18)$$

where $(dx/dt)_{exp}$ and $(dx/dt)_{calc}$ are the experimentally measured, and the calculated reaction rates, respectively, at the same degree of conversion, and n are the number of calculated and measured points used for the fitting. Given that the fitting is performed on reaction rate with respect to conversion rather than on conversion with respect to temperature/time, the effect of an induction period i.e. due to the slow activation of the reaction not be properly accounted for. In addition, in the above expression there is no reaction rate at the beginning of the reaction. Therefore, integration would only be valid above a certain threshold value of conversion.

In the present work, the kinetic model of the different stages of the dual-curing system are analyzed independently. It will be considered, like in the isoconversional analysis, that the activation of the second curing stage is independent from the completion of the first one. Again, this means that the slow activation of BG is taking place during the first curing process.

For the first curing stage, equations (17) and (18) are used. In order to ensure that the resulting rate expression can be integrated properly, it will be assumed that the first of the autocatalytic elements will be, in fact, a n-th order element, that is, $m_1 = 0$.

For the second curing stage, equations (17) and (18) are used in order to determine the kinetic parameters of the different autocatalytic elements. However, activation of the second process is delayed due to the latent character of BG. For the analysis of this delayed activation, we will assume the validity of isoconversional hypotheses during the activation period. Assuming also that the second process is independent from the first one, the existence of a pre-curing period, and that the delayed activation is better reflected by dynamic data, we can write the following:

$$I_2(x_{act}) = \frac{g(x_{act})}{k_{0,act}} - I_1(x_{act}) = \int_0^{t_{act}} exp\left(-\frac{E_{act}}{R}\cdot\frac{1}{T}\right)\cdot dt = \frac{1}{\beta}\cdot\frac{E_{act}}{R}\cdot p(y_{act}) \qquad (19)$$

Where $g(x_{act})$ is the integral form of the kinetic model function $f(x)$ at the activation degree of conversion x_{act}, E_{act} is the activation energy corresponding to this period, $k_{0,act}$ is the pre-exponential factor, $y_{act} = {E_{act}}/{R\cdot T_{act}}$, T_{act} is the temperature at the defined x_{act}, and $p(y)$ is the 4th order Senum-Yang approximation [18] of the temperature integral or the Starink approximation. The parameters ${g(x_{act})}/{k_{0,act}}$ and E_{act} are assumed to be constant during the activation period.

We can consider that, for $x < x_{act}$, the conversion is given by

$$x \approx x_{act}\cdot\frac{\int_0^t exp\left(-{E_{act}}/{R\cdot T}\right)\cdot dt}{I_2(x_{act})} \qquad (20)$$

Therefore, the reaction rate ${dx}/{dt}$, for $x < x_{act}$ can be estimated as:

$$\frac{dx}{dt} \approx x_{act} \cdot \frac{exp\left(-E_{ind}/R \cdot T\right)}{I_2(x_{act})} \qquad (21)$$

Note that expressions (20) and (21) are strictly valid for the analysis of the activation period after the pre-curing period. Keeping in mind that we want to analyze the process starting from the preparation of the fresh formulation, one should use $g(x_{act})/k_{0,act} = I_2(x_{act}) + I_1(x_{act})$ instead of $I_2(x_{act})$. In addition, the value of x_{act} should be sufficiently small so as to minimize the error in the calculation of a fictional rate dx/dt during this activation period. For $x > x_{act}$,we can consider that the reaction rate dx/dt is represented correctly by eq. (17).

3.2 Simulation of dual-curing processes

Isoconversional-based simulation

Simulation of dual-curing processes is possible starting from isoconversional integral data, as reported in the literature [14].

Simulation of the first process of the dual-curing system can be easily performed under isothermal conditions by means of eq. (6) and making use of the parameters $g_1(x_1)/k_{0,1,x}$ and $E_{1,x}$ for each degree of conversion x_1. Simulation of dynamic curing experiments at constant heating rates can be performed using eq. (7) and the parameters $g_1(x_1)/k_{0,1,x}$ and $E_{1,x}$, by numerical iteration of the temperature $T_{1,x}$ for a given degree of conversion x_1 at the desired heating rate β.

Simulation of the second process of the dual-curing system can be performed assuming that the pre-curing is already over. In this case, isothermal simulation is performed using eq. (6) and the parameters $E_{2,x}$ and $I_2(x_2)$ (instead of $g_2(x_2)/k_{0,2,x}$) for each degree of conversion x_2. The same applies to the simulation of dynamic curing experiments using eq. (7). If one wanted to simulate the second process starting from the fresh, uncured

formulation (i.e. for the simulation of the global curing process [14]), isothermal simulation is performed using eq. (6) and the parameters $E_{2,x}$ and $g_2(x_2)/k_{0,2,x}$, and dynamic simulation is performed using eq. (7) and the same parameters $E_{2,x}$ and $g_2(x_2)/k_{0,2,x}$.

A global conversion of epoxy groups, x_{epoxy}, can be calculated taking into account the composition of the formulation (see Table 1) as

$$x_{epoxy} = 0.4 \cdot x_1 + 0.6 \cdot x_2 \qquad (22)$$

Although both curing stages are analyzed independently, it will be assumed, for the isoconversional-based simulation, that $x_{epoxy} = 0.4 \cdot x_1$ during the first curing stage and that $x_{act} = 0.4 + 0.6 \cdot x_2$ during the second curing stage.

Model-based simulation

Simulation of the first curing process is performed by numerical integration of eq. (17), under isothermal or nonisothermal temperature programmes. It is considered that the first of the autocatalytic elements is a n-th order element, that is, $m_1 = 0$.

Simulation of the second curing process can be performed assuming that the pre-curing is already over. This is accomplished by numerical integration of eq. (21) during the activation period (corresponding to the slow release of the initiator) and, once it is over, making use of eq. (17). If one wanted to simulate the second process starting from the fresh, uncured formulation (i.e. for the simulation of the global curing process), the activation of the latent initiator should be performed by numerical integration of eq. (21) but making use of $g(x_{act})/k_{0,act} = I_2(x_{act}) + I_1(x_{act})$ instead of $I_2(x_{act})$. Once the activation period is over, simulation of the rest of the process is carried out by numerical integration of eq. (17). Because of this activation period, it is not necessary that the first of the autocatalytic elements in eq. (17) be of a n-th order type.

A global conversion of epoxy groups, x_{epoxy}, can be calculated using eq. (22), after numerical integration of x_1 and x_2 using the corresponding rate expressions for dx_1/dt and dx_2/dt. Accordingly, an overall reaction rate can be calculated using the folowing expression.

$$\frac{dx_{epoxy}}{dt} = 0.4 \cdot \frac{dx_1}{dt} + 0.6 \cdot \frac{dx_2}{dt} \quad (23)$$

Note that, because the rate expressions are integrated independently, this allows for some overlapping of the first and second curing process at some point, depending on the temperature programming.

4 RESULTS AND DISCUSSION

4.1 Preliminary analysis

Figure 1 compares the dynamic curing at 2, 5 and 10 ºC/min of a fresh dual formulation. It can be observed that the curing process takes place in two well-separated and defined curing stages. The first stage corresponds to an epoxy-amine addition (see Scheme 2), involving the reaction of primary and secondary amine groups. The reaction is autocatalytic due to the activation of the epoxy ring by proton donors or other activating species [27] such as the hydroxyl groups formed in the course of the reaction, although in reality the reaction mechanism is more complex and involves the formation a number of reactive and non-reactive complexes [27-30]. The second curing process corresponds to the epoxy homopolymerization of the epoxy groups in excess after the thermal decomposition of BG leading to the release of the initiator (see Scheme 3) [2, 14]. A more detailed description of the epoxy homopolymerization mechanism can be found in the literature [23, 31].

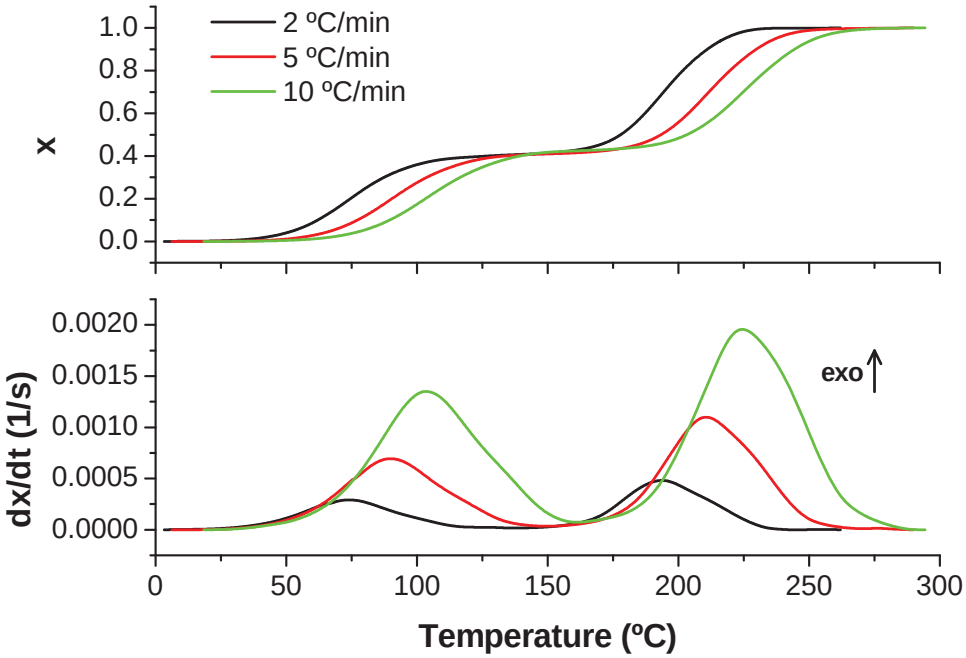

Figure 1: Comparison of the conversion (upper graph) and rate curves (lower graph) corresponding to the dynamic curing at 2, 5 and 10 ºC/min of the system under study.

a. Primary amine reaction

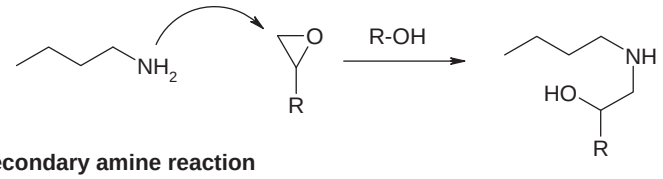

b. Secondary amine reaction

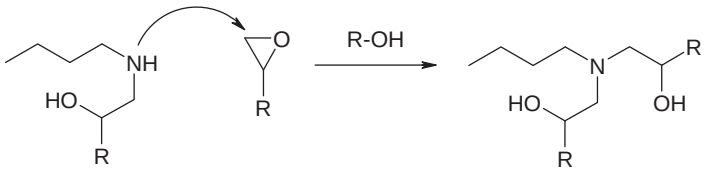

Scheme 2: Epoxy-amine reaction.

a. Thermal decomposition of BG

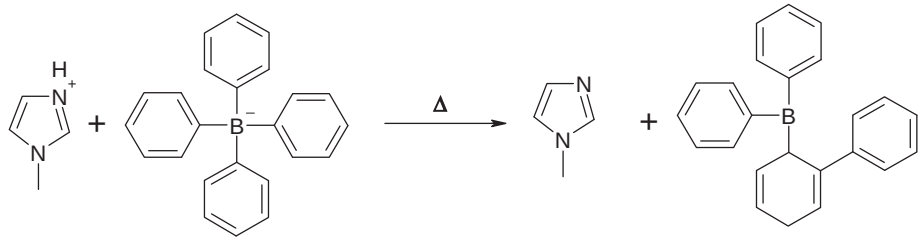

b. Anionic epoxy homopolymerization

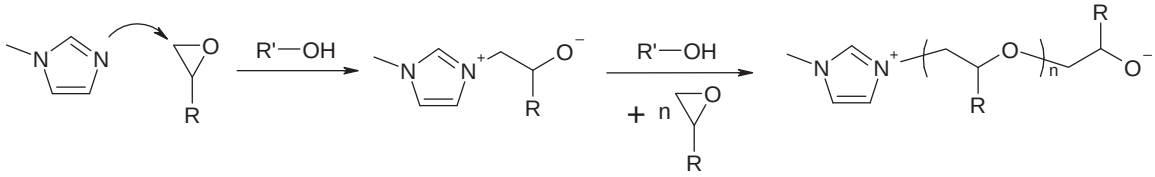

Scheme 3: Thermal decomposition of BG (a) and anionic epoxy homopolymerization (b).

In contrast with our previous study using Jeffamine as crosslinking agent for the first curing stage [2, 14], it can be observed in Figure 1 that the curing stages using DETA show an almost perfect separation. Moreover, this is also much better than other sequential dual-curing processes with controlled thermal activation such as off-stoichiometric thiol-epoxy formulations [23], or other epoxy systems [13]. In fact, an apparent separation was reported by Sun et al. [13], but in their work the contribution of the second curing process was very small, while in the present work the contributions of the first and second curing processes are more balanced (Figure 1). Although the reaction kinetics of the second curing stage does depend on the state of completion of the first curing stage, that is, the presence of hydroxyl groups formed as a consequence of the epoxy-amine reaction (Scheme 2), from a practical point of view, both processes can be considered independent, as discussed in our previous work [14]. This is evident from Figure 1 which shows there is little or no overlapping at all between the curing processes.

The average reaction heat of all dynamic experiments was 462 J/g or 93.8 kJ/ee. This is very close to the reference value of 100 kJ/ee for epoxy-amine and epoxy homopolymerization [2, 27, 32, 33]. The formulation was prepared using an amine-epoxy ratio of 0.4, which is in agreement with the contribution of the first curing process to the total reaction heat.. Therefore, in spite of the uncertainty in the determination of the baseline and integration of the reaction peaks, it can be concluded that both reaction processes take place quantitatively, as was reported also in our previous studies [2].

In Table 2 we report the glass transition temperatures of the uncured formulation, the intermediate material and the fully cured material. It can be observed that the intermediate material has a near-ambient T_g, similar to our previous work [2], but the T_g of the fully cured material is 138 ºC. This could be expected because the final T_g of stoichiometric DGEBA-DETA formulations is about 135 ºC [33] and that of the DGEBA homopolymer with 4 phr of BG is 132 ºC [2]. In fact, the value is somewhat higher than expected (i.e. using Fox equation) but it might be that the neat epoxy homopolymer is not completely cured due to topological restrictions. However, such discrepancies are within experimental error.

Table 2: Glass transition temperatures (T_g) and heat capacity step during relaxation (ΔC_p) of the uncured, intermediate and fully cured materials.

	T_g (ºC)	$\Delta C_p (kJ/kg \cdot K)$
Uncured	-16	0.56
Intermediate	29	0.55
Cured	138	0.24

Another remarkable feature is the fact that the heat capacity step (ΔC_p) during the glass transition of the uncured and intermediate materials are 0.56 and 0.55, respectively. These significantly similar values suggest that there is minimal crosslinking during this first curing stage. According to Hale et al. [34], the change in glass transition should be linear with respect to conversion before gelation takes place, because the change in T_g is mainly associated with a decrease in free volume of the system. The ratio between the ΔC_p of the intermediate and uncured materials gives a parameter λ that is very close to 1. This parameter λ is used in some theoretical $T_g - x$ relationships [35, 36], and its value close to unity indicates an almost linear increase in T_g with conversion x. Assuming that the DGEBA-DETA polycondensation is nearly ideal from a network build-up point of view [37], we can use the well-known Flory-Stockmayer equation [38] for the prediction of conversion at gelation. Taking into account the amine-epoxy equivalent ratio of 0.4, (see Table 1) and that the functionality of DETA is 5, one can predict an epoxy conversion at the gel point equal to 0.32. This is very close to the conversion at the end of the first curing process. Taking into account the epoxy excess, this implies that the behavior of

458 the system is almost liquid-like throughout the first curing process, in agreement with the
459 experimental results.
460
461 The good separation between processes prompted us to perform a preliminary kinetics
462 analysis of the curing process. In the present work, we carried out an isoconversional
463 analysis of the global data using the integral method proposed by Starink, given by eq.
464 (9) and parameters $A = 1.0008$, $B = -0.312$ and $k = 1.92$ [19]. The results of the
465 analysis are shown in Figure 2. It can be observed a clear difference between the kinetic
466 parameters below and above conversion 0.4. At lower degrees of conversion, values of
467 E_x of about 55 kJ/mol are obtained. Above, the values of E_x are around 90 kJ/mol. These
468 values are in good agreement with previously reported results [12, 14]. A clear transition
469 is observed, with peak E_x values higher than 150 kJ/mol. In spite of the uncertainty in
470 the analysis in this region (as deduced from the error bars in the figure), this transition
471 can be attributed to the activation of the latent thermal initiator BG for the second curing
472 stage. This is also an indication of a highly latent behavior in the intermediate state, which
473 was confirmed experimentally for a similar system employing the same base [2]. The
474 application of the advanced isoconversional method of Vyazovkin, making use of the 4th
475 order approximation of Senum and Yang, produced identical results to those shown in
476 Figure 2. This is because, in the experimental range, the values of $y = E/R \cdot T$ are around
477 20-35 and, in this region, the Starink method produces an error lower than 0.2 % in the
478 temperature integral $p(y)$ and lower than 0.1 % in the determination of E [19].

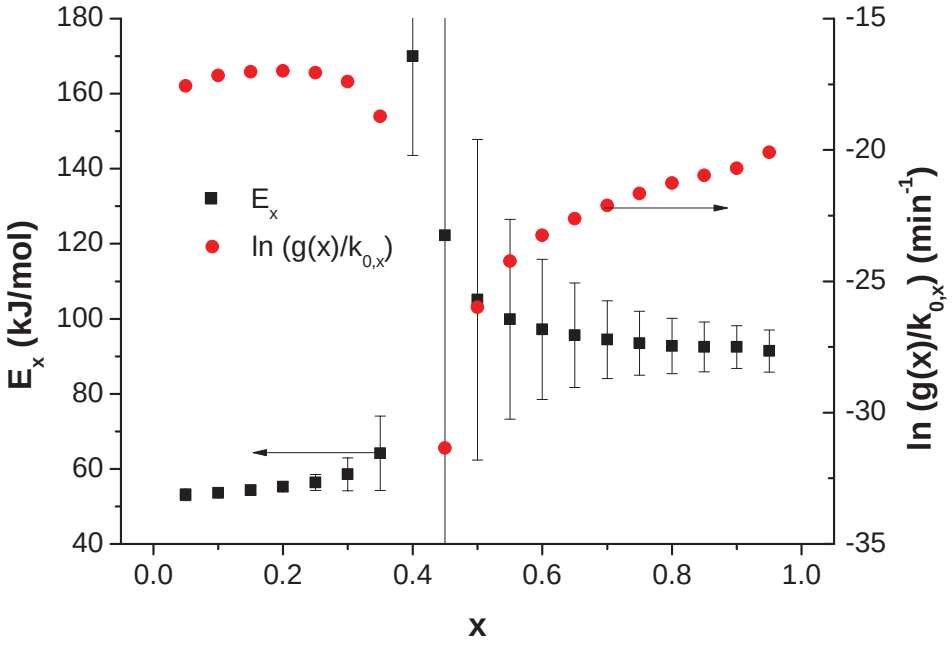

Figure 2: Results of the isoconversional kinetics analysis of the global dynamic experiments in Figure 1, using eq. (9).

Using the data in Figure 2, we simulated the isothermal curing at different temperatures using eq. (6). A tentative selection of curing temperatures for the first curing process ranged from 70 to 100 ºC, while the second curing process could be analyzed from temperatures of 150 ºC to 210 ºC.

In the subsequent kinetics analysis of the curing process, the different curing stages will be analyzed separately. We will take into account that the activation of the second curing reaction is independent from the first curing process. According to the methodology explained in section 3.1, the whole of the second curing process is regarded as independent from the first curing process, but in reality this is not strictly true. However, this hypothesis will be valid as long as the second curing process (or the majority of it) takes place once the first curing process is over.

4.2 Detailed kinetics analysis

Figure 3 shows the conversion and rate curves corresponding to the first curing process of the dual-curing system, carried out isothermally at temperatures from 70 to 100 ºC in 10 ºC steps. The evolution of conversion and rate curves with temperature follows the

expected trends. In none of the cases it was observed further reaction beyond the stabilization of the isothermal baseline at the end of the first curing process. The rate curves have an autocatalytic character, as expected for epoxy-amine curing. The average reaction heat of the different experiments was 193.4 J/g or 39.3 kJ/ee. These values agree with the theoretical reaction heat of about 100 kJ/ee for epoxy groups and the composition of the formulation (see Table 1). This could be expected taking into account our previous results in a similar system [2, 14]. If the curves in Figure 3 are compared with previously reported data [14], it can be observed that the first stage, corresponding to the epoxy-amine addition, is much faster in the present case in which DETA is the amine, than in previous works with Jeffamine curing agent [14]. This is due to the decelerating effect produced by polyether structure of Jeffamine, as reported by Swier et al. [30].

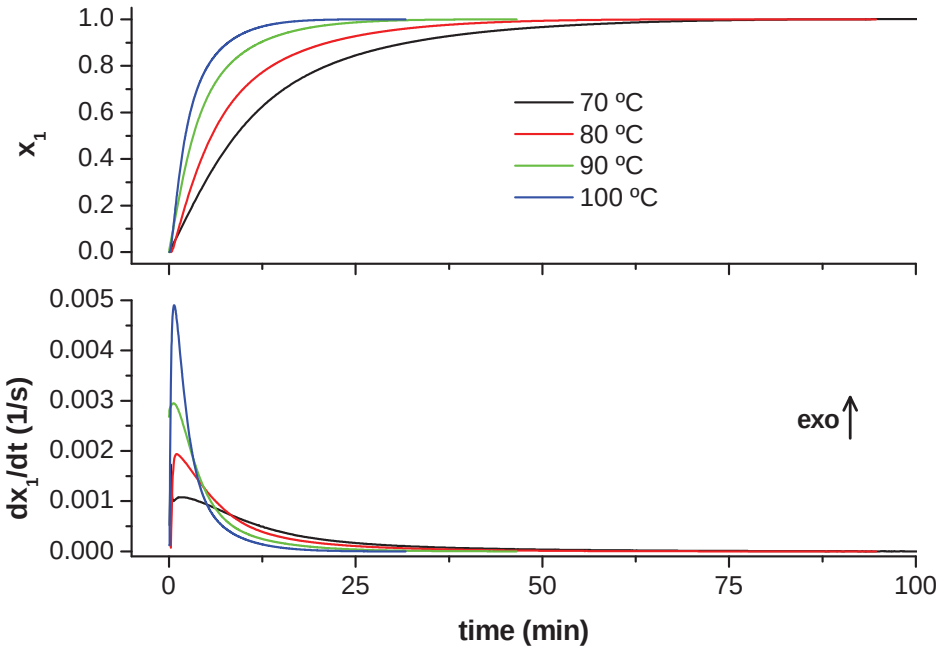

Figure 3: Conversion x and rate dx/dt for the 1st curing process of the dual-curing system at different temperatures.

Figure 4 shows the conversion and rate curves corresponding to the second curing process of the dual-curing system, after a precuring at 90 ºC for 40 minutes, carried out isothermally at temperatures from 150 to 210 ºC in 10 ºC steps. The evolution of conversion and rate curves with temperature follow the expected trends. The average reaction heat of the different experiments was 281.2 J/g or 57.1 kJ/ee, which suggests that the excess epoxy groups after the first curing process react completely during the second

curing process, as reported previously [2, 14]. Taking into account the reaction times and temperatures, one can notice a significant difference in reaction rates between the second (Figure 4) and first curing processes (Figure 3), as was foreshadowed by the preliminary dynamic analysis (Figure 1).

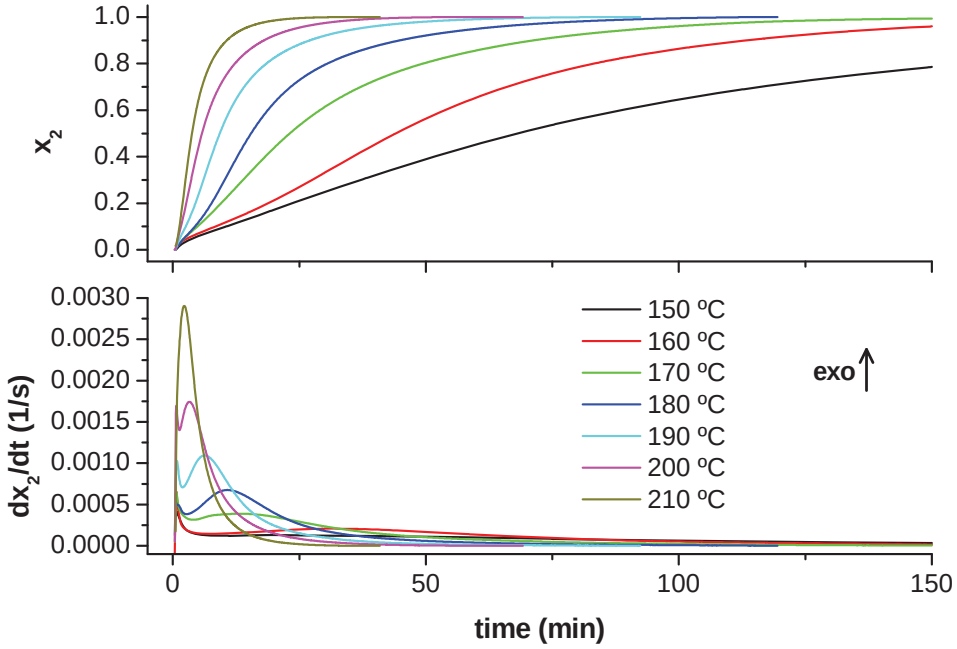

Figure 4: Conversion x and rate dx/dt for the 2nd curing process of the dual-curing system at different temperatures.

Upon close examination of Figure 4, one can observe that, at the beginning of the curing exotherms, there is a sharp peak that can be associated with the thermal decomposition of the latent initiator and the activation of the second curing process. This was also observed in our previous study [14]. However, given the sharpness of this first peak, there is some uncertainty as to the true contribution of this small peak and to the possibility of obtaining reliable kinetic information at the beginning of the second curing process using only isothermal data. For that purpose, a number of dynamic experiments were carried out, after a precuring at 90 ºC for 40 minutes, in order to observe in more detail the activation of the second curing process. Figure 5 shows the conversion and rate curves at 2.5, 5 and 10 ºC/min. The activation of the second process is observed as a small exothermic event starting around 100-120 ºC, followed by the exotherm corresponding to the second curing process at temperatures higher than 150 ºC. It should also be noted that, for this second curing process, the reaction kinetics are faster in the present work, with DETA as first-

stage curing agent, than in our previous works [2, 14] with Jeffamine. This may be caused by the effect of the polyether structure of the Jeffamine curing agent on some of the reaction steps of the epoxy homopolymerization involving the participation of 1MI.

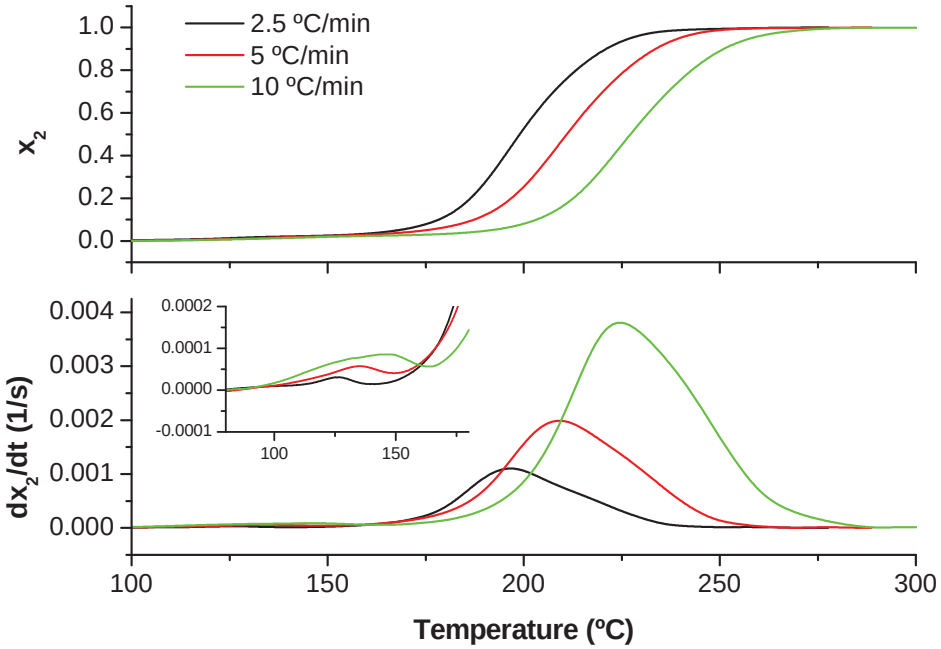

Figure 5: Conversion x and rate dx/dt for the 2nd curing process of DGDETA_0.4_BG4 at different heating rates. The inset shows the detail of the activation of the latent thermal base.

The kinetics analysis of the first curing process was performed using only isothermal data but, for the second curing process, both isothermal and nonisothermal data were combined in order to obtain the kinetic parameters. The results of the integral isoconversional analysis are shown in Figure 6. In agreement with the preliminary kinetics analysis (Figure 2) and our previous work [14], there is a clear difference between the apparent activation energies of the first and second curing process, respectively. The values are rather constant except at the beginning of both the first and second curing stages, which may be caused by experimental error at the beginning of the measurement, especially in the case of the second curing process, given the uncertainty in the kinetics and thermal effect of the activation of the latent base. Overall, the values agree well with those previously reported [12, 14].

With regards to the second curing process, a very small difference between the values of $I_2(x_2)$ and $g_2(x_2)/k_{0,2,x}$ is observed. This can be explained by the low value of the

precuring factor I_1, which is logical taking into account that precuring was carried out at 90 ºC for 40 minutes only, and the large difference in reactivity between the first and second curing process.

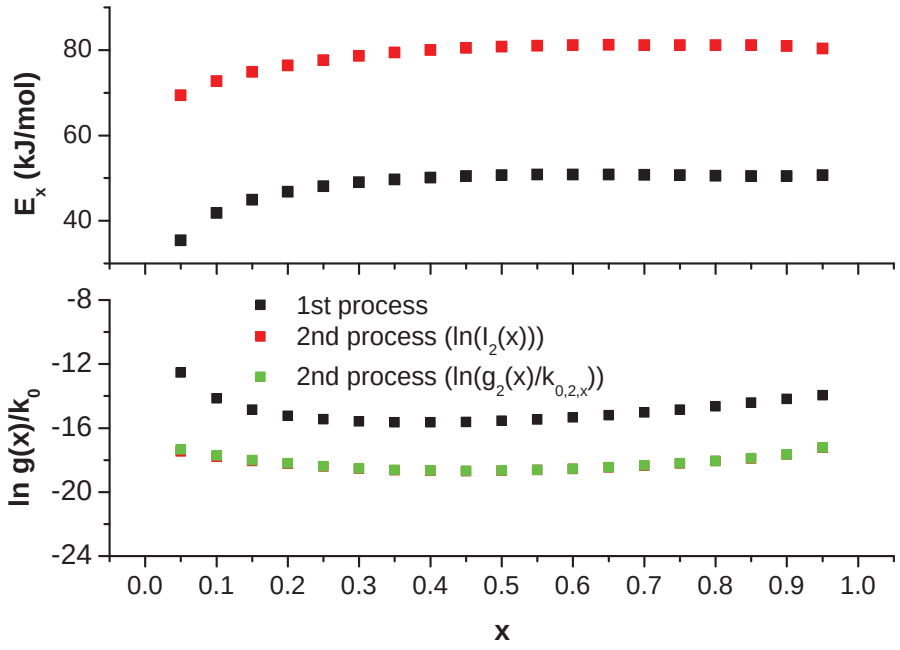

Figure 6: Results of the isoconversional analysis of the 1st and 2nd curing processes.

The results of the model-fitting analysis of the first curing process are shown in Figure 7 and Table 3. It can be seen that the experimental curves are properly fitted using the empirical model given by eq. (17) with two autocatalytic elements, each one with their kinetic constant k_i and reaction orders m_i and n_i. The use of more autocatalytic elements did not further improve the quality of the adjustment. The activation energy of both kinetic constants agree well with the evolution of the apparent activation energy resulting from the isoconversional analysis (see Figure 6). That is to be expected, since they should ensure a proper modelling of the temperature-dependence of the curing process. The values of reaction orders m_i and n_i reported in Table 3 reflect the typical autocatalytic character of epoxy-amine polycondensation reactions. However, it must be acknowledged that their values are somewhat arbitary, since they are mainly used as fitting parameters that are able to reproduce the shape of the curing exothem. As noted by Flammersheim [29], the quality of the fitting can improve when using kinetic models with empirical parameters, but their physical meaning is lost. Mechanism-based modelling [27-30] was not considered in the present work.

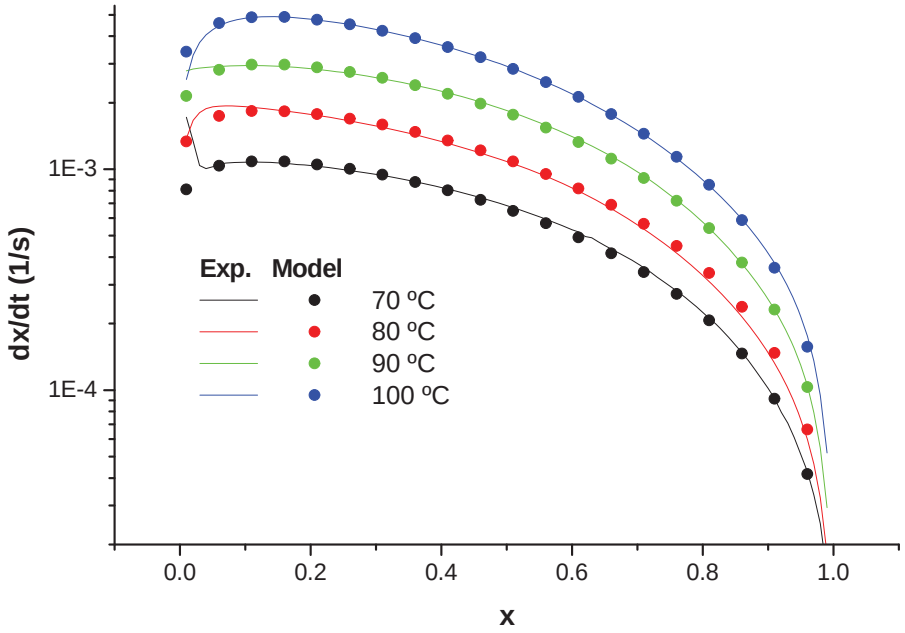

Figure 7: Fitting of the experimental isothermal curves of the first curing process to the kinetic model given by eq. (17).

Table 3: Kinetic parameters for the kinetic model of the first curing process (eq. (17))

	$i = 1$	$i = 2$
$E_i(kJ/mol)$	45.37	55.17
$ln\,(k_{0,i})\,(s^{-1})$	8.14	12.98
m_i	0	0.325
n_i	0.771	1.752

Figure 8 and Table 4 show the results of the model-fitting analysis of the second curing process. Experimental curves could be properly fitted using the empirical model given by eq. (17), but using in this case up to four autocatalytic elements, owing to the more complex shape of the curing exotherms. Given the wide range of experimental temperatures and heating rates used, the agreement between the model predictions and the experimental data is remarkable. Some noticeable discrepancies are observed at the beginning of the isothermal experiments but, overall, the temperature dependence ant the shape of the curves is well predicted. With regards to the values of the kinetic parameters, the obtained activation energies are also in good agreement with the previous

isoconversional analysis, although this analysis reveals a somewhat more complex temperature dependence. Like in the previous case, it should be acknowledged that the reaction orders m_i and n_i are fitting parameters that are mainly responsible for the adjustment of the shape of the curing exotherms, and therefore they have very little or no physical meaning at all. Indeed, some of the values reported in Table 4 are highly unrealistic from a physical point of view.

The activation parameters were obtained, however, only from the dynamic data, since it was considered that the beginning of the isothermal data was quite unreliable. A value of $x_{act} = 0.005$ was considered.

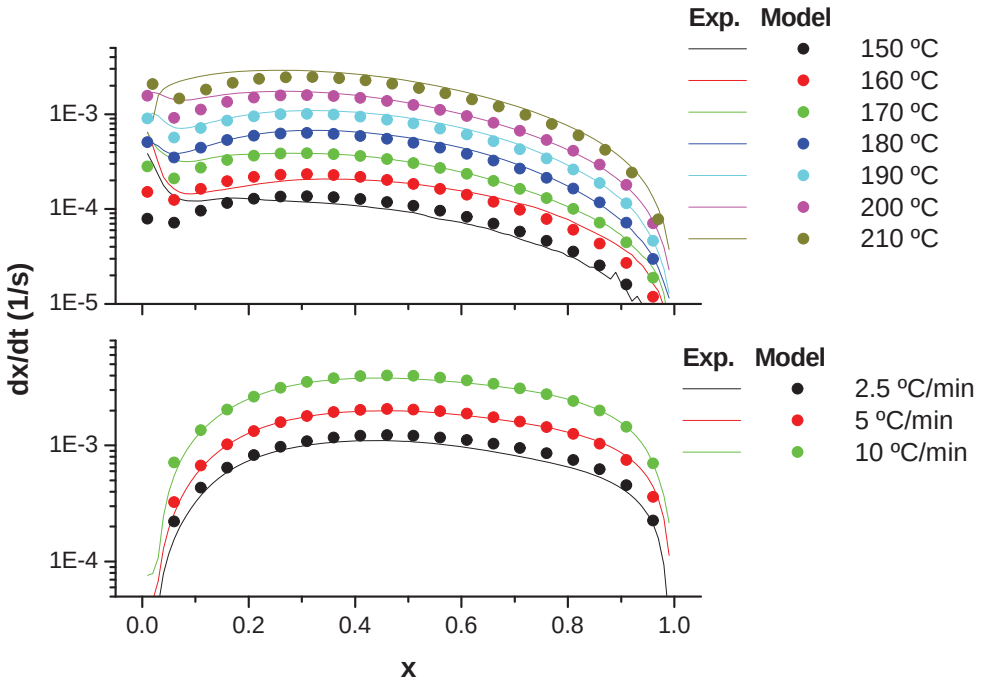

Figure 8: Fitting of the experimental isothermal (upper graph) and dynamic (lower graph) curves of the second curing process to the kinetic model given by eq. (17).

Table 4: Kinetic parameters for the kinetic model of the second curing process (eqs. (17) and (21))

$x < x_{act}$	$E_{act}(kJ/mol)$	149.42			
	$g(x_{act})/k_{0,act}\ (min)$	-44.19			
	$I_2(x_{act})\ (min)$	-44.41			
		$i = 1$	$i = 2$	$i = 3$	$i = 4$
$x \geq x_{act}$	$E_i(kJ/mol)$	102.32	81.32	55.43	87.13
	$ln\ (k_{0,i})\ (s^{-1})$	20.04	15.88	3.55	17.57
	m_i	0.047	0.817	2.647	8.893
	n_i	42.346	1.907	0.103	1.641

4.3 Kinetic modeling validation

The results of both the isoconversional and model-fitting approaches can be validated by comparing the resulting $x - t$ or $x - T$ predictions with the experimental data.

Figure 9 shows that both isoconversional data and the kinetic model can be used to reproduce the experimental curves of the first curing process almost perfectly, without significant differences between the different approaches.

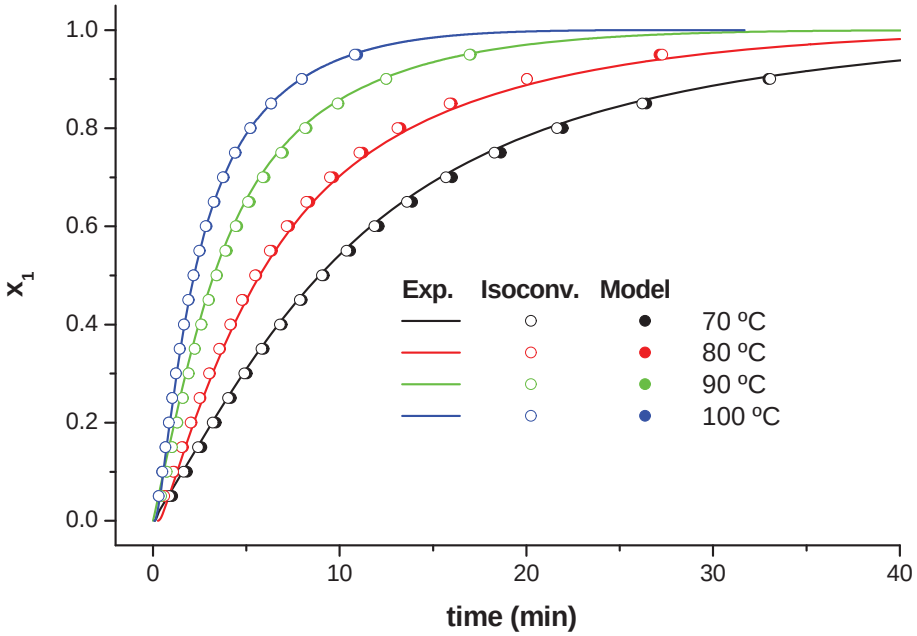

Figure 9: Simulation of the isothermal curves of the first curing process using the isoconversional parameters (open symbols) and the kinetic model (closed symbols), and comparison with experimental data (lines).

The same applies to the second curing process, as seen in Figure 10. With regards to the isoconversional analysis, it should be noted that we used $E_{2,x}$ and $I_2(x_2)$ (instead of $g_2(x_2)/k_{0,2,x}$) for the simulation of isothermal and dynamic data using eqs. (6) and (7), respectively, because we are comparing the simulations with the experimental curves after the precuring period. Minor differences between the results of both methodologies are observed mainly at the beginning of the second curing process, because in the isoconversional analysis all the curves were used, while in the case of the kinetic model all the curves were used to determine kinetic parameters using eq. (17), but only the dynamic curves were used for the analysis of the activation period. Again, E_{act} and $I_2(x_{act})$ was used instead of $g(x_{act})/k_{0,act}$ for the simulation of the activation periodusing eq. (21). In all cases, the agreement between simulated and experimental data was remarkable, especially taking into consideration experimental uncertainty.

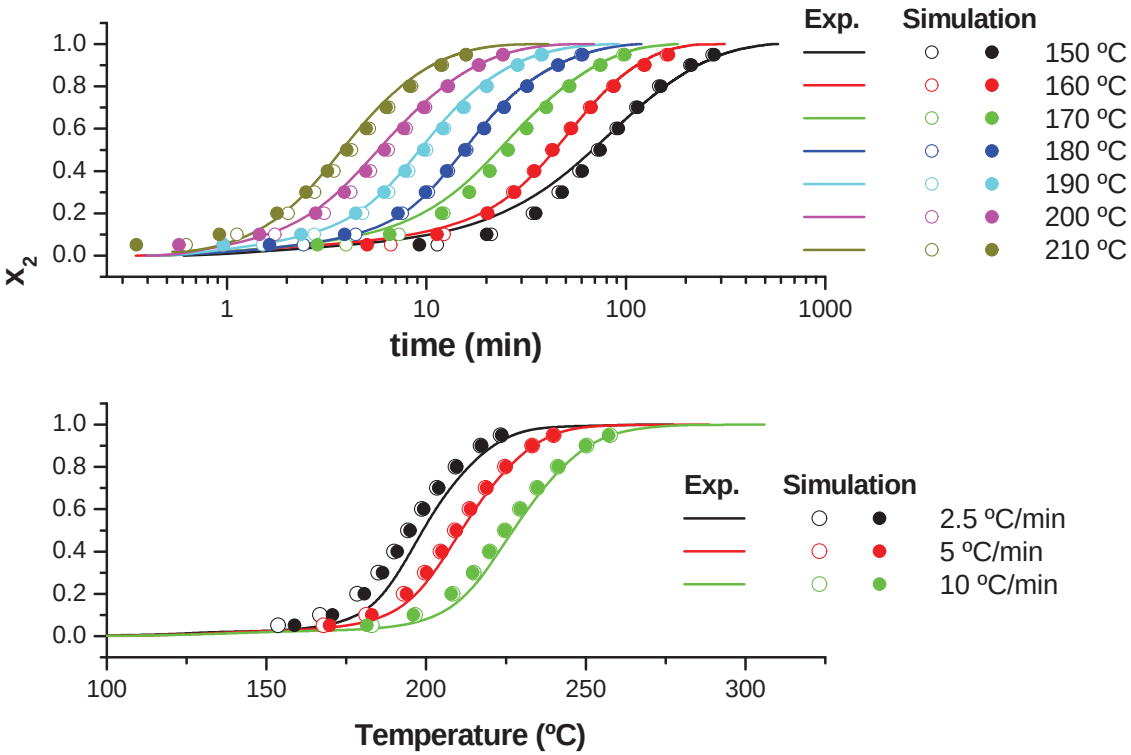

Figure 10: Simulation of the isothermal (upper graph) and dynamic (lower graph) curves of the second curing process using the isoconversional parameters (open symbols) and the kinetic model (closed symbols), and comparison with experimental data (lines).

Now, it would be good to see if the kinetic parameters of the first and second curing process could be used to simulate a global curing process, and compare it with experimental data. Since we have already shown the global curing curves at different heating rates (see Figure 1), we will first simulate the dynamic data. In Figure 11 we compare the experimental data at 10 ºC/min with the simulation using the model parameters in Table 3 and Table 4. The second curing process has been simulated from the beginning of the heating process; the slow activation period has been simulated using $g(x_{act})/k_{0,act}$ instead of $I_2(x_{act})$ in eq. (21) and, once this is over, eq. (17) has been used. Little discrepancies are observed in the rate curves but, taking into account experimental uncertainty, the overall agreement between the simulated and the experimental data is excellent, especially with regards to the $x - T$ curve. The simulation also reveals there is some little overlapping between the first and second curing processes. However, given that the overlap starts at the very end of the first curing process, its effect is negligible

from a practical point of view. Therefore, we can assume that the employed methodology, based on the independent analysis of each curing process, is valid.

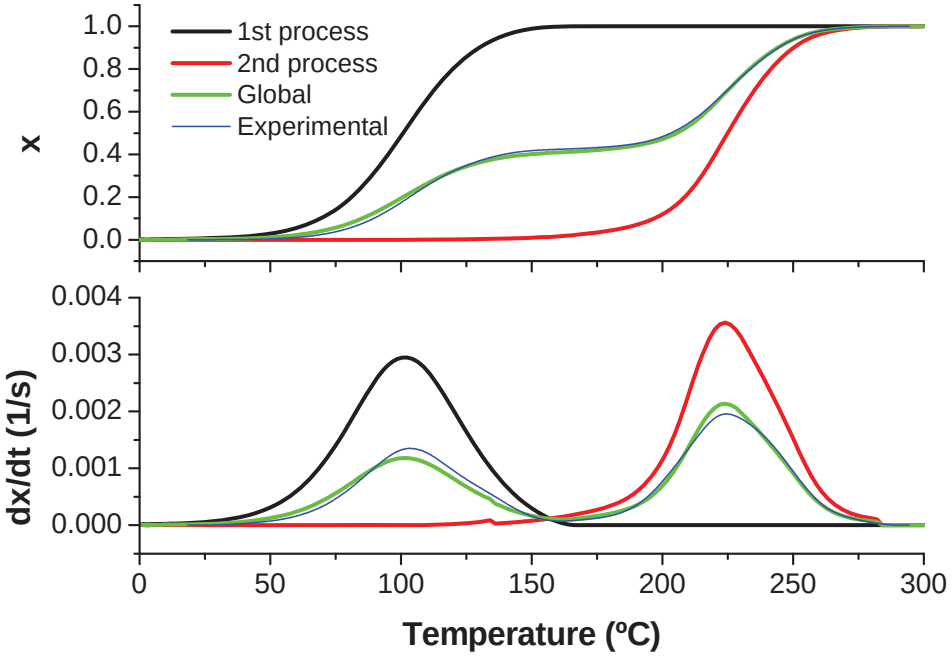

Figure 11: Simulation of the conversion and rate curves corresponding to the global curing process using the kinetic model at 10 ºC/min, and comparison with experimental data.

In Figure 12 we compare $x - T$ curves of the three dynamic experiments at 2, 5 and 10 ºC/min (from Figure 1) with the simulated curves using isoconversional data and the kinetic model. The simulation using the kinetic model has been performed as stated before. For the isoconversional simulation of the experimental curves, we have used eq. (7) and isoconversional parameters $E_{1,x}$ and $g_1(x_1)/k_{0,1,x}$ for the first curing process, and $E_{2,x}$ and $g_2(x_2)/k_{0,2,x}$ for the second curing process (assuming independent activation of both curing processes). Taking into account experimental uncertainty, the simulated data produces very close results to the experimental ones, as seen before. Both isoconversional and the kinetic model produce almost identical results; some differences are only noticed at the beginning of the first and second curing process, and low heating rates.

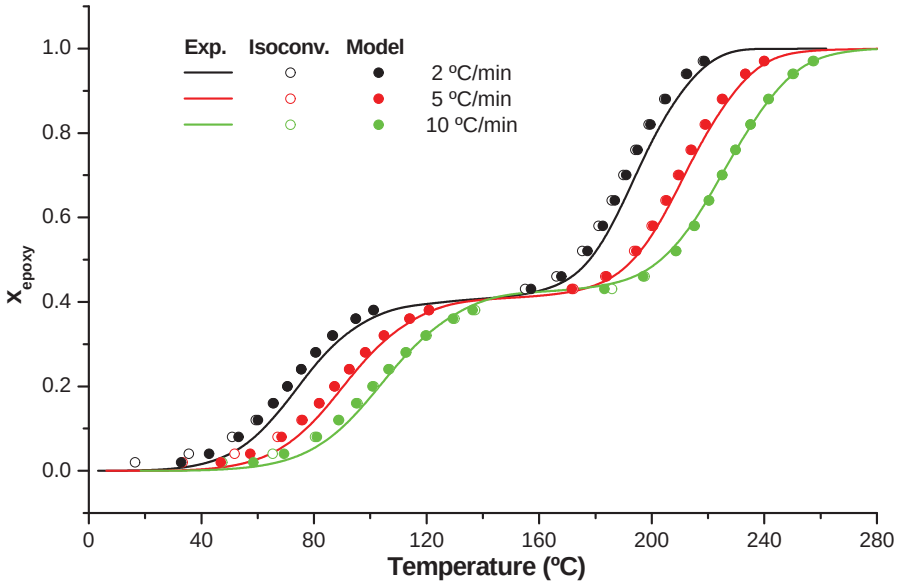

675

676 Figure 12: Simulation of the conversion curves corresponding to the global curing process at different
677 heating rates using the isoconversional parameters (open symbols) and the kinetic model (closed symbols),
678 and comparison with experimental data (lines).

679

680 The isoconversional data and the kinetic model were also used to simulate the isothermal
681 curing process at different temperatures, shown in Figure 13. The simulations have been
682 carried out following the same criteria as before. In the case of isoconversional data,
683 simulations have been performed using eq. (6) instead of eq. (7). The highest temperature
684 used, 160 ºC, is within the range of the experimental data for the second curing process
685 but is an extrapolation for the first curing process. The lowest temperature used, 100 ºC,
686 is within the range of the experimental data for the first curing process but is an
687 extrapolation for the second curing process. In the case of 120 and 140 ºC, the results are
688 an extrapolation outside the experimental range for both curing process. It should be noted
689 that the curing process would be incomplete at 100 and 120 ºC, because the ultimate T_g
690 of this dual system is 140 ºC and vitrification would take place.

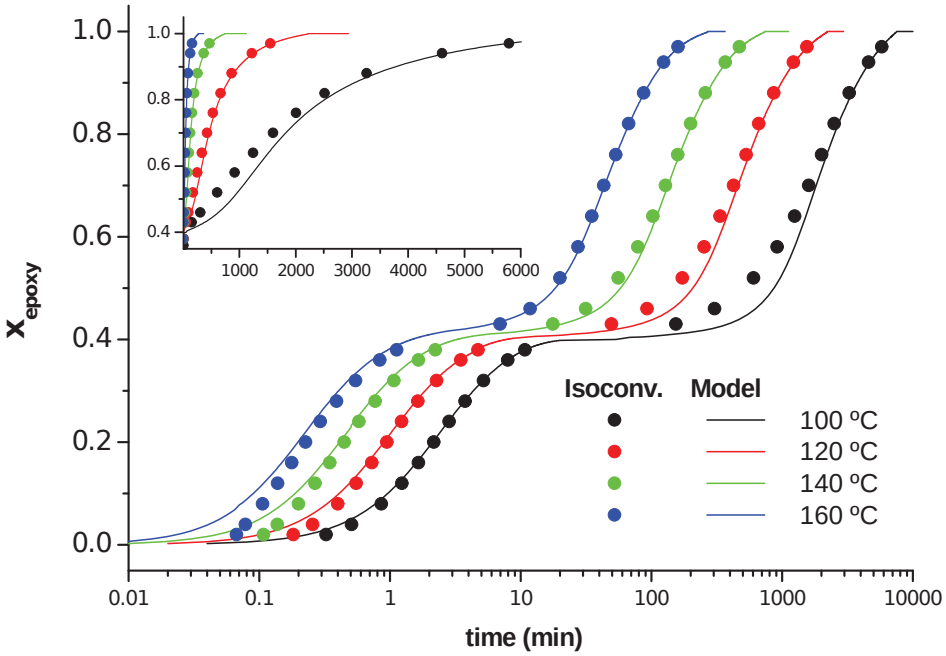

Figure 13: Simulation of the conversion curves corresponding to the global curing process at different isothermal temperatures using the isoconversional parameters (closed symbols) and the kinetic model (lines). The inset shows a detail of the $x - t$ curves at degrees of conversion higher than 0.4 and time in normal scale (instead of $\log_{10}$ scale as in the main graph).

The large difference in reactivity between the first and second curing stages, of about two decades in reaction time, can be noticed in Figure 13. Isoconversional and kinetic model results yield, overall, very similar results, especially at 100 and 120 ºC for the first curing process, and at temperatures of 160 and 140 ºC for the second curing process. Differences become apparent when the extrapolated temperatures are farther away from the experimental data. The kinetic model predicts somewhat higher intermediate stability than the isoconversional data. However, the inset shows that, in reality, these differences are minor. They might be caused, in part, by the experimental uncertainty in the determination of conversion at the beginning of the second curing process under isothermal conditions (see Figure 4 and accompanying discussion) and the fitting of the model (see Figure 8). In any case, all these results are subject to extrapolation error; long-term behavior at lower temperatures should be analyzed using a different experimental setup. Some differences are also observed at the beginning of the first curing process, but the effect is not relevant, given the short timescale in which they are observed.

The above results have shown that it is possible to use either isoconversional methods or kinetic modeling methods for the analysis and simulation of curing processes under a variety of isothermal and nonisothermal conditions. Isoconversional analysis does not require the determination of a model, and therefore the kinetic parameters are determined in a more straightforward manner and simulations are faster and easier, from a computational point of view, especially when the temperature profiles are well defined (isothermal, dynamic, combinations of steps [14]), which is to be expected in applications where heat accumulation is negligible due to good dissipation (i.e. thin films). However, kinetics analysis based on model fitting produce a set of parameters that allows a more flexible utilization in terms of simulation, for instance the curing of thick composites where accumulation of heat and temperature overshoots can take place. Choice of either method or the other depends on convenience rather than accuracy, since both can provide comparatively good results.

An alternative to kinetic modeling is the use of differential isoconversional methods based on eq. (3), taking natural logarithms [17]. The advantage of such approach is the simplicity in the determination of kinetic parameters E_x and $ln(k_{0,x} \cdot f(x))$ just by linear regression throughout the entire conversion range. Simulation is performed by numerical integration of eq. (3), and by interpolation of E_x and $ln(k_{0,x} \cdot f(x))$ data in a table. Simulation of curing processes using differential isoconversional data produces results that are comparable to those obtained by model fitting and integral isoconversional methods, but this analysis has been excluded from the present work for simplicity purposes. Whichever the method, the results are dependent only on the quality of the experimental data used, as long as it is applied in a proper and consistent way.

4. CONCLUSIONS

The curing kinetics of a dual-curing system combining amine-epoxy polycondensation with homopolymerization of excess epoxy groups, using a latent thermal initiator, has been studied.

The study of the global curing process under nonisothermal conditions evidenced the difference in curing kinetics of both curing stages. Isoconversional kinetics analysis revealed the existence of separate levels of apparent activation energy corresponding to the amine-epoxy polycondensation (lower value and lower curing temperatures) and the homopolymerization of epoxy groups (higher value and higher curing temperatuers).

The kinetics of both curing processes were investigated separately using isoconversional integral methods and model-fitting methodology. It was assumed that the slow activation of the latent thermal initiator, used for the second curing stage, was independent from the completion of the first curing process. Isoconversional and model-fitting methodologies produced comparable and consistent results, as expected, since they were applied in a consistent way for the analysis of kinetic data and subsequent simulation.

The global curing process could be simulated successfully using isoconversional and model-fitting data. Isothermal simulation of the global process evidenced the significant difference in reaction time, about two decades, between the first and second curing processes. It could also simulate the stagnant conversion in between the two curing processes, making possible the design of controlled curing schedules with good intermediate stability.

Choice of isoconversional or model-fitting methods for analysis and simulation depends only on the processing scenario to be considered. Isoconversional methods are sufficient to simulate curing processes with controlled temperature profiles, while kinetic modeling is more suitable for the more flexible simulation of processing scenarios where deviations from the temperature programme may take place.

5. ACKNOWLEDGEMENTS

The authors would like to thank MINECO (Ministerio de Economía, Industria y Competividad) (MAT2017-82849-C2-1-R and MAT2017-82849-C2-2-R) and Generalitat de Catalunya (2017-SGR-77 and Serra Húnter programme) for the financial support.

REFERENCES

[1] X. Ramis, X. Fernández-Francos, S. De La Flor, F. Ferrando, À. Serra, Click-based dual-curing thermosets and their applications (chapter 16), in: Q. Guo (Ed.) Thermosets 2nd edition: Structure, Properties and Application, Elsevier, 2017.

[2] A.O. Konuray, N. Areny, J.M. Morancho, X. Fernández-Francos, À. Serra, X. Ramis, Preparation and characterization of dual-curable off-stoichiometric amine-epoxy thermosets with latent reactivity, Polymer, 146 (2018) 42-52.

[3] D.P. Nair, N.B. Cramer, J.C. Gaipa, M.K. McBride, E.M. Matherly, R.R. McLeod, R. Shandas, C.N. Bowman, Two-Stage Reactive Polymer Network Forming Systems, Advanced Functional Materials, 22 (2012) 1502-1510.

[4] A. Belmonte, X. Fernàndez-Francos, À. Serra, S. De la Flor, Phenomenological characterization of sequential dual-curing of off-stoichiometric thiol-epoxy systems: Towards applicability, Materials & Design, 113 (2017) 116-127.

[5] F. Saharil, F. Forsberg, Y. Liu, P. Bettotti, N. Kumar, F.N. Haraldsson, W.v. derWijngaart, K.B. Gylfason, Dry adhesive bonding of nanoporous inorganic membranes to microfluidic devices using the OSTE(+) dual-cure polymer, Journal of Micromechanics and Microengineering, 23 (2013) 025021.

[6] G. Gonzalez, X. Fernandez-Francos, A. Serra, M. Sangermano, X. Ramis, Environmentally-friendly processing of thermosets by two-stage sequential aza-Michael addition and free-radical polymerization of amine-acrylate mixtures, Polymer Chemistry, 6 (2015) 6987-6997.

[7] S. Chatani, C. Wang, M. Podgórski, C.N. Bowman, Triple Shape Memory Materials Incorporating Two Distinct Polymer Networks Formed by Selective Thiol-Michael Addition Reactions, Macromolecules, 47 (2014) 4949-4954.

[8] W. Xi, H. Peng, A. Aguirre-Soto, C.J. Kloxin, J.W. Stansbury, C.N. Bowman, Spatial and Temporal Control of Thiol-Michael Addition via Photocaged Superbase in Photopatterning and Two-Stage Polymer Networks Formation, Macromolecules, 47 (2014) 6159-6165.

[9] A.O. Konuray, F. Liendo, X. Fernández-Francos, À. Serra, M. Sangermano, X. Ramis, Sequential curing of thiol-acetoacetate-acrylate thermosets by latent Michael addition reactions, Polymer, 113 (2017) 193-199.

[10] O. Konuray, X. Fernández-Francos, X. Ramis, À. Serra, State of the art in dual-curing acrylate systems, Polymers, 10 (2018).

[11] J.A. Carioscia, J.W. Stansbury, C.N. Bowman, Evaluation and control of thiol-ene/thiol-epoxy hybrid networks, Polymer, 48 (2007) 1526-1532.

[12] J.M. Morancho, X. Ramis, X. Fernández-Francos, J.M. Salla, A.O. Konuray, À. Serra, Curing of Off-Stoichiometric Amine-Epoxy Thermosets, Journal of Thermal Analysis and Calorimetry, 133 (2018) 519-527.
[13] H. Sun, Y. Liu, Y. Wang, H. Tan, Curing Behavior of Epoxy Resins in Two-Stage Curing Process by Non-Isothermal Differential Scanning Calorimetry Kinetics Method, Journal of Applied Polymer Science, 131 (2014).
[14] N. Areny, O. Konuray, X. Fernàndez-Francos, J.M. Salla, J.M. Morancho, X. Ramis, Time-temperature-transformation (TTT) diagram of a dual-curable off-stoichiometric epoxy-amine system with latent reactivity, Thermochimica Acta, 666 (2018) 124-134.
[15] X. Sun, J.P. Gao, Z.Y. Wang, Bicyclic Guanidinium Tetraphenylborate: A Photobase Generator and A Photocatalyst for Living Anionic Ring-Opening Polymerization and Cross-Linking of Polymeric Materials Containing Ester and Hydroxy Groups, Journal of the American Chemical Society, 130 (2008) 8130-8131.
[16] T. Rodima, I. Kaljurand, A. Pihl, V. Mäemets, I. Leito, I.A. Koppel, Acid-Base Equilibria in Nonpolar Media. 2.1 Self-Consistent Basicity Scale in THF Solution Ranging from 2-Methoxypyridine to EtP1(pyrr) Phosphazene, The Journal of Organic Chemistry, 67 (2002) 1873-1881.
[17] S. Vyazovkin, N. Sbirrazzuoli, Isoconversional kinetic analysis of thermally stimulated processes in polymers, Macromolecular Rapid Communications, 27 (2006) 1515-1532.
[18] L.A. Pérez-Maqueda, J.M. Criado, The Accuracy of Senum and Yang's Approximations to the Arrhenius Integral, Journal of Thermal Analysis and Calorimetry, 60 (2000) 909-915.
[19] M.J. Starink, The determination of activation energy from linear heating rate experiments: a comparison of the accuracy of isoconversion methods, Thermochimica Acta, 404 (2003) 163-176.
[20] S. Vyazovkin, D. Dollimore, Linear and nonlinear procedures in isoconversional computations of the activation energy of nonisothermal reactions in solids, Journal of Chemical Information and Computer Sciences, 36 (1996) 42.
[21] S. Vyazovkin, Evaluation of activation energy of thermally stimulated solid-state reactions under arbitrary variation of temperature, Journal of Computational Chemistry, 18 (1997) 393-402.
[22] S. Vyazovkin, Modification of the Integral Isoconversional Method to Account for Variation in the Activation Energy, Journal of Computational Chemistry, 22 (2001) 178-183.
[23] X. Fernandez-Francos, A.-O. Konuray, A. Belmonte, S. De la Flor, A. Serra, X. Ramis, Sequential curing of off-stoichiometric thiol-epoxy thermosets with custom-tailored structure, Polymer Chemistry, 7 (2016) 2280-2290.

[24] A.O. Konuray, X. Fernandez-Francos, X. Ramis, Analysis of the reaction mechanism of the thiol-epoxy addition initiated by nucleophilic tertiary amines, Polymer Chemistry, 8 (2017) 5934-5947.
[25] N. Boyard, A. Millischer, V. Sobotka, J.L. Bailleul, D. Delaunay, Behaviour of a moulded composite part: Modelling of dilatometric curve (constant pressure) or pressure (constant volume) with temperature and conversion degree gradients, Composites Science and Technology, 67 (2007) 943-954.
[26] P.I. Karkanas, I.K. Partridge, Cure modeling and monitoring of epoxy/amine resin systems. I. Cure kinetics modeling, Journal of Applied Polymer Science, 77 (2000) 1419-1431.
[27] B.A. Rozenberg, Kinetics, Thermodynamics and Mechanism of Reactions of Epoxy Oligomers with Amines, Advances in Polymer Science, 75 (1986) 113-165.
[28] S. Swier, G. Van Assche, B. Van Mele, Reaction kinetics modeling and thermal properties of epoxy-amines as measured by modulated-temperature DSC. I. Linear step-growth polymerization of DGEBA + aniline, Journal of Applied Polymer Science, 91 (2004) 2798-2813.
[29] H.J. Flammersheim, Kinetics and mechanism of the epoxide-amine polyaddition, Thermochimica Acta, 310 (1998) 153-153.
[30] S. Swier, G. Van Assche, W. Vuchelen, B. Van Mele, Role of Complex Formation in the Polymerization Kinetics of Modified Epoxy-Amine Systems, Macromolecules, 38 (2005) 2281-2288.
[31] X. Fernandez-Francos, W.D. Cook, A. Serra, X. Ramis, G.G. Liang, J.M. Salla, Crosslinking of mixtures of DGEBA with bislactone initiated by tertiary amines. IV. Effect of hydroxyl groups on initiation and curing kinetics, Polymer, 51 (2010) 26-34.
[32] K.J. Ivin, in: J. Brandrup, E.H. Immergut (Eds.) Polymer Handbook, Wiley, New York, 1975.
[33] D. Santiago, X. Fernàndez-Francos, X. Ramis, J.M. Salla, M. Sangermano, Comparative curing kinetics and thermal-mechanical properties of DGEBA thermosets cured with a hyperbranched poly(ethyleneimine) and an aliphatic triamine, Thermochimica Acta, 526 (2011) 9-21.
[34] A. Hale, C.W. Macosko, H.E. Bair, Glass transition temperature as a function of conversion in thermosetting polymers, Macromolecules, 24 (1991) 2610-2621.
[35] J.P. Pascault, R.J.J. Williams, Glass transition temperature versus conversion relationships for thermosetting polymers, Journal of Polymer Science, Part B: Polymer Physics, 28 (1990) 85-95.
[36] R.A. Venditti, J.K. Gillham, Relationship between the glass transition temperature (Tg) and fractional conversion for thermosetting systems, Journal of Applied Polymer Science, 64 (1997) 3-14.

[37] X. Fernández-Francos, X. Ramis, Structural analysis of the curing of epoxy thermosets crosslinked with hyperbranched poly(ethyleneimine)s, European Polymer Journal, 70 (2015) 286-305.
[38] J.P. Pascault, H. Sautereau, J. Verdu, R.J.J. Williams, Thermosetting polymers, Marcel Dekker, New York [etc.] :, 2002.